

Massive Data-Centric Parallelism in the Chiplet Era

Marcelo Orenes-Vera, Esin Tureci, David Wentzlaff, Margaret Martonosi
Princeton University, Princeton, New Jersey, USA
{movera, esin.tureci, wentzlaf, mrm} @princeton.edu

Abstract

Recent works have introduced task-based parallelization schemes to accelerate graph search and sparse data-structure traversal, where some solutions scale up to thousands of processing units (PUs) on a single chip. However, parallelizing these memory-intensive workloads across millions of cores requires a scalable communication scheme as well as designing a cost-efficient computing node that makes multi-node systems practical, which has not been addressed in previous research.

To address these challenges, we propose a task-oriented scalable chiplet architecture for distributed execution (Tascade), a multi-node system design that we evaluate with up to 256 distributed chips—over a million PUs. We introduce an execution model that scales to this level via proxy regions and selective cascading, which reduce overall communication and improve load balancing. In addition, package-time reconfiguration of our chiplet-based design enables creating chip products optimized post-silicon for different target metrics, such as time-to-solution, energy, or cost.

We evaluate six applications and four datasets, with several configurations and memory technologies, to provide a detailed analysis of the performance, power, and cost of data-centric execution at a massive scale. Our parallelization of Breadth-First-Search with RMAT-26 across a million PUs—the largest of the literature—reaches 3021 GTEPS.

1. Introduction

In the last decade, we have seen the rise of massive many-core systems [12, 27, 84, 35, 14] that target AI workloads via dataflow computation. There is, however, still an unmet demand for systems that can massively accelerate applications that utilize sparse data structures [29].

Recent works have proposed task-based parallelization schemes that accelerate graph and sparse data traversal by splitting the program at irregular memory accesses [58, 17, 63, 71], offering a promising path for parallelizing these communication- and data-intensive applications. While some solutions (e.g. Dalorex [63]) scale up to thousands of processing units (PUs) on-chip, the challenge of parallelizing these applications across millions of cores has not been tackled.

Starting with a tile-based architecture, in order to achieve such scaling, one must address the following challenges: (1) *Scalable long-distance communication*: Due to the irregular nature of the communication in graph applications, the larger the number of processing elements, the higher the average communication distance. This increases both latency and contention on the network. (2) *Work imbalance*: Because of

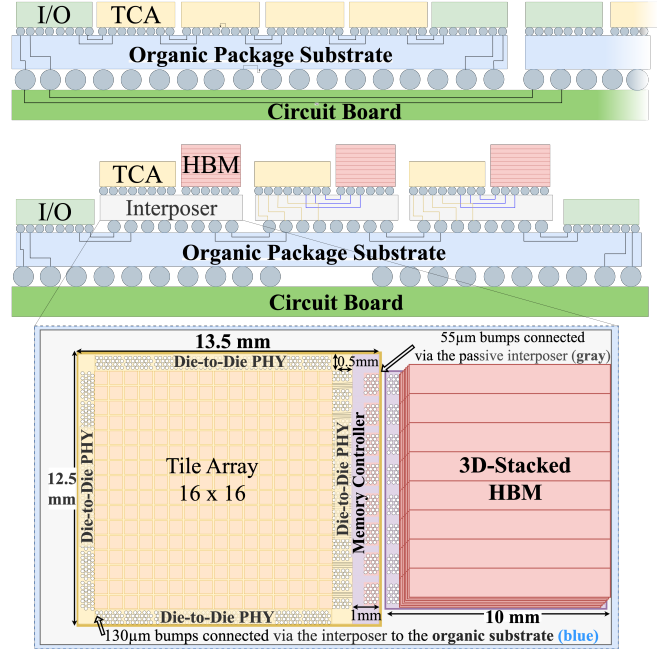


Figure 1: Two possible integrations of Tascade. Top: two packages on a board, each featuring only tiled-compute array (TCA) dies, optimized for time-to-solution as it maximizes parallelization (lower data footprint per die). Bottom: a single package with TCA dies and stacked DRAM, optimized for performance-per-watt/\$ (§5).

the power-law distribution of many graphs, growing dataset sizes result in a growing number of edges for a small number of vertices. When parallelizing across more cores, this, in turn, results either in serialization due to atomics and coherence overheads (e.g. in do-all parallelization schemes) and/or work imbalance (e.g. single-owner-per-data parallelization scheme by Dalorex) when scaling out. (3) *Energy, performance, and cost efficiency trade-offs*: Building a system with millions of cores requires the design of a multi-node system that brings with it various additional design and performance constraints. In order to fully analyze trade-offs of energy, performance, and cost efficiency, a detailed architectural design of a full multi-node system with complete communication primitives for fine-grained messages across multiple chips is necessary.

These challenges have not been addressed so far with previous studies on accelerating sparse and graph applications. Even for the manycore systems that are currently available, we lack detailed studies of large system-design tradeoffs.

Our approach: We present a multi-node architecture for massively parallel execution of sparse and graph applications. Our task-oriented scalable chiplet architecture for distributed execution system (Tascade), overcomes the above limitations

by: (a) utilizing an atomic-free data-local execution model that utilizes proxy ownership of data, relaxing the *single-owner-per-data* constraint employed by Dalorex by allowing proxy tiles to merge updates to data owned by distant tiles—thereby reducing work-imbalance and network traffic; (b) designing a scalable system with nodes composed of grids of tiled compute array (TCA) chiplets, optionally interleaved with DRAM as shown in Fig. 1; and (c) studying tradeoffs in cost, performance, and energy of packaging-time design decisions.

We evaluate strong scaling performance when parallelizing sparse applications with up to one million processors across 256 nodes, with no dataset preprocessing or partitioning.

Proxy Regions and Selective Cascading: Tascade shards the dataset across the tile grid allocated to run a program, similar to Dalorex. In addition, to reduce long-distance communication, Tascade divides the tile grid into subgrids. In each subgrid, each tile is assigned proxy ownership to a chunk of data as if the entire data array were distributed only within this subgrid. Proxy owners are permitted to cache an update to remotely stored/owned original data. From here on in this paper, we call the tile that owns the original data array chunk the “owner tile” to distinguish it from the proxy owners. Tasks requiring long-distance communication are first sent to a proxy owner within the sender’s region. If an update needs to be sent to the owner tile eventually, additional proxy owners en route may also process the task as proxy tasks. This is triggered opportunistically: the system moves the invocations to the owner tile directly when no network traffic is present in order to minimize staleness but utilizes all available proxy owners when they are idle, and there is network traffic. When applied to tasks that perform associative operations, this results in accumulating updates in a cascading manner and filtering out otiose invocations at the owner tile, significantly reducing the average communication distance of task invocations (see §5). This dynamic approach also improves work balance and network contention, as many of the task invocations targeting a tile that owns very hot data are filtered out by the proxy tiles.

Scalable System Design: Designing systems composed of millions of cores is only practical if cost constraints are taken into account. We investigated the fabrication cost of data-local architectures like Dalorex and found that the granularity of SRAM per tile affects key metrics of throughput and energy efficiency per dollar. Using these metrics, we studied pre-silicon and packaging-time choices—not done in previous studies. Because fabricating separate silicon masks for different target metrics is expensive, we propose a composable architecture where crucial decisions like on-chip memory capacity or off-chip bandwidth are made after silicon fabrication. Fig. 1 depicts two packaging options where the same TCA dies are integrated to create different chip products, each optimized for a different metric. A TCA die may be attached to a DRAM device during packaging. This effectively increases the capacity of a tile’s *local memory* since the DRAM storage exclusively assigned to the tiles of the adjacent TCA die.

The technical contributions of this paper are:

- Software-reconfigurable proxy ownership and dynamic selective cascading that allow aggregation of updates from distant tiles efficiently, which improves work balance and reduces network contention.
- A scalable architecture where chip design decisions such as on-chip memory, # of PUs, network topology and off-chip bandwidth are made post-silicon.
- A viable path for interleaving any # of columns of compute and DRAM chiplets on a chip package.
- A detailed study of tradeoffs in cost, performance, and energy efficiency of several package designs.

We evaluate Tascade and demonstrate that:

- Tascade exhibits strong scaling up to 1 million PUs, while prior work starts to plateau after thousands.
- The proxy region improve performance by $2.6\times$ geomean over Dalorex [63] for 64x64 (single chip package), and by $3.3\times$ geomean when scaling to larger grid.
- Optimized task scheduling and buffering improve the overall system’s throughput up to $4.7\times$.
- Different packaging options of Tascade lead to different optimal design points for key metrics in HPC, such as energy efficiency and throughput per unit cost.
- Our BFS parallelization is $3.4\times$ faster than the most performant entry of the Graph500 list for RMAT-26, and $5.2\times$ faster for RMAT-22.

2. Background and Motivation

Memory accesses at graph and sparse linear algebra applications do not exhibit spatial or temporal locality, resulting in poor cache behavior and intense traffic in the memory hierarchy [50]. Prior work aiming to accelerate these workloads mitigate memory latency via decoupling, prefetching, and hardware pipelining techniques [83, 61, 28, 74, 65, 2, 57, 58, 17, 71, 33]. Fifer [58] and Polygraph [17] increase utilization further through spatiotemporal parallelization, while Hive [71] provides ordered parallelization. However, all of these works store the dataset on off-chip DRAM; thus, their scalability is limited by the network and memory bandwidth. Tesseract [4] and GraphQ [93] tackle this problem via processing-in-memory. However, their proposed integration of PUs on the logic layer of a memory cube [70] is less scalable than the manycore integration proposed by Dalorex [63].

We detail the data-local execution model of Dalorex in §2.1 since this paper extends this model to improve work balance and network contention, as well as to design a more practical system integration. We then review the latest manycore architectures in §2.2 with a focus on chip manufacturing.

2.1. The Data-Local Execution Model

Tasking and queuing: In Dalorex, the original program is split into tasks that are executed at the tile co-located with the memory region that the task operates on. A task can spawn its dependent tasks by injecting inputs for each task in the

Reconfigurable Aspects / Prior Work	Memory Capacity on package	#Processing Elements on package	Configurable Network Topology	Software ISA Programmable Processors
Fifer [21]	✓	✗	✗	✗
Tesseract [4],GQ [93]	✓	✗	✗	✓
Dalorex [63]	✗	✗	✗	✓
PolyGraph [17]	✓	✗	✗	✗
Decades [8, 23]	✗	✗	✗	✓
ESP [25]	✗	✗	✗	✓
Manticore [91]	✓	✗	✗	✓
Intel’s PIUMA [1]	✓	✗	✗	✓
Graphcore [39]	✗	✗	✓	✓
Sambanova [20]	✓	✓	✓	✗
Cerebras [12]	✗	✗	✓	✓
Groq [27]	✗	✗	✗	✓
Tesla Dojo [27]	✓	✓	✗	✓
Esperanto [21]	✗	✗	✗	✓
Google TPU [35]	✓	✗	✓	✗
Nvidia A100 [14]	✓	✗	✗	✓
Tascade	✓	✓	✓	✓

Table 1: Post-silicon configurability of the on-chip network topology, memory capacity and # of processing elements (PEs) per chip package, and whether the PEs can execute software instructions.

output queue (OQ) of the tile it is executed at, which drains into a logical network channel. At each tile, there is one input queue (IQ) per task type for incoming task invocations. An IQ is populated with invocation parameters that are either (a) directly pushed by a prior task executed in the local tile, or (b) coming as task messages from the network channels.

Task prioritization: In Dalorex, work efficiency and PU utilization are highly impacted by the order of task executions. The task scheduling unit (TSU) determines the order of execution of tasks based on the occupancy of queues. It prioritizes tasks whose IQ is highly populated, or OQ is empty. The TSU “senses” the network pressure and executes tasks that will relieve pressure when it is high (IQs full) or increase when it is low (OQs rarely pushing). Tascade uses *reconfigurable queue sizes*, which §5.2 demonstrates to be beneficial since different applications perform best with distinct queue sizes.

Distant task communication: A program in data-local execution is a sequence of tasks invoking other tasks upon pointer indirection, with no concept of execution threads (no main task). Thus, spawned tasks may target any random tile in the grid, i.e., whoever owns the data to be processed next. As the size of the grid increases, so would the average number of router hops of a task message and, thus, the network contention. Tascade introduces *proxy ownership* (see §3.1) which relaxes the constraint of *single-owner-per-data* in Dalorex. §5.3 shows how proxy improves performance by reducing the excessive traffic occurring in large tile grids.

Tile grid and network routing: The size of the grid a program runs on is determined by the user at compile time. Thus, the logical tile ID is microcoded when a workload is selected

to run on a given grid, and it is used for XY routing. Since the dataset is statically partitioned across the tiles on the grid, and the first parameter of a task message is a global index to a data array, this index is used to route the message, avoiding message headers altogether. Based on the size of the array associated with a network channel for routing purposes, the router selects the bits that indicate the destination tile ID. Tascade supports *selective cascading* by allowing proxy tiles to grab task messages despite not being the destination tile.

2.2. Fabrication Cost of Manycore Systems

In recent years, the widespread demand for large deep-learning models has accelerated the development of manycore and dataflow systems that can massively parallelize compute-intensive workloads. Although the demand for graph and sparse linear algebra workloads is growing, we have not seen systems exhibiting as high strong-scaling performance as dense systems due to their irregular data-access patterns and low arithmetic intensity (ops/byte).

Table 1 shows a selection of the recent manycore systems where the upper ones focus on sparse workloads and the rest focus on AI. While some of these manycores have good attributes for sparse data processing (large on-chip SRAM capacity [63, 62, 27, 39, 84] or on-package DRAM [14, 20, 35, 91, 4]), the ratio of memory capacity and PUs is optimized for dense computation, and the interconnect is designed for dataflow communication. For our work, instead of designing a manycore architecture with a memory-to-PU ratio and network optimized solely for sparse data, we propose a chiplet architecture where these can be configured at chip packaging time; we evaluate them of in §5.4 also considering cost-effectiveness.

Packaging-time configurability for better silicon reuse: The semiconductor industry is increasingly utilizing having multiple dies in a chip package [46, 56, 26, 5, 82] to reduce fabrication costs and enable reusing components across different products. From the silicon manufacturing perspective, the Non-Recurring-Engineering (NRE) cost of a wafer mask is so high with respect to the silicon wafer itself that the cost per wafer is $18\times$ larger when manufacturing 100 wafers, instead of 100,000 [34]. Since the volume of silicon production of each chip architecture generation is not as high in the HPC market as in the consumer electronic market, we argue that the mass fabrication of a chiplet that serves as a building block for scalable architectures is a valuable proposition. Thus, we designed a chiplet that can be fabricated at high volume to amortize NRE costs, and then integrated into a Multi-Chip Module (MCM) package as an arbitrary grid of dies. Fig. 1 shows that Tascade allows integrating DRAM between columns of TCA dies (and not just on the chip edges as in prior work).

3. The Tascade Approach

§3.1 describes how Tascade overcomes the scalability challenges of prior work through proxy ownership and selective cascading. Tascade also offers several *software-configurable*

features that can be tuned for each application and task to optimize performance. Particularly, §3.2 presents these features for task scheduling, queue sizes and Network-on-Chip (NoC), while §3.3 describes our approach for caches and prefetching, and Table 2 summarizes the remaining configurable knobs. §3.4 introduces our *package-time configurable* design and provides a thorough discussion of some packaging options.

3.1. Proxy Owners and Selective Cascading

Programs that can be parallelized for loop iterations have the underlying assumption that the order of iterations, as well as interleavings of operations across different iterations, preserves correctness. Many graph and sparse applications have commutative operations, making them amenable to such parallelization, provided that all writes to the same data are atomic. This is the underlying power of models such as Bulk-Synchronous Parallelization (BSP) to guarantee eventual correctness allowing interleavings of all other read/write operations. Distributed-memory MapReduce [18] implementations may avoid atomic operations by updating copies of the result array and merging them at the end. However, since pre-merge computations and merging cannot be effectively overlapped in such software schemes, it leads to idle PUs. This under-utilization is exacerbated in the context of BSP, where each epoch has a barrier. The data-local programming model proposed by Dalorex eliminates the need for atomic updates with a *single-owner-per-data* task-based model. However, large parallelizations using this model suffer from work imbalance as only a single tile’s PU can operate on a given data, and work-per-data is highly skewed.

Tascade relaxes the single-owner-per-data constraint of Dalorex and employs *two modes of data ownership*. (1) *Original data owner*: As in Dalorex, dataset arrays are sharded as equal-sized chunks to tiles, where each tile *owns* a chunk of each data array; (2) *Proxy data owner*: We allocate *proxy regions* by subdividing the tile grid into smaller regions. For selected tasks, we distribute the proxy ownership of copies of the data array(s) across the tiles of *each* proxy region, such that the most recent updates coming from within the region can be stored in the tile’s proxy cache (P\$, detailed in §3.3). Proxy regions allow intermediary storage to perform reduction operations of remote data through *proxy tasks*. So, in addition to commutativity, Tascade leverages the *associativity* in BSP operators: data updates are merged in any combination with eventually correct convergence.

Applicability: Fig.2 explains how proxy regions are configured in software. Each proxy region is responsible for a copy of a dataset array. Any task in the data-local execution model can have a proxy task. In our evaluation (§5), we apply this to the vertex update task of graph applications and the reduction phase of the histogram and sparse algebra workloads. Proxy tasks can be applied to read-only data as well as to modifiable arrays. For the latter, aggregated data updates are eventually sent to the owner, resulting in eventual consistency. Fig.2

depicts this scenario with two proxy tasks (T3’) being invoked on the same tile, coming from different T2 tasks.

Hardware support for reduction operations: Data updates to a proxy tile eventually trigger a task invocation towards the owner tile. This happens transparently to software, thanks to the write-back P\$. When a P\$ cacheline is evicted, the data is ‘written-back’ by invoking another proxy task in the direction of the owner tile. For that, the P\$, similarly to the PU, has the ability to push into the OQs. This hardware support enables Tascade to keep the perks of Dalorex’s single-owner-per-data task model while improving work-balance by allowing multiple tiles to perform updates. Moreover, since Tascade enables overlapping updates to proxy P\$s with merges with the original data array, it avoids the synchronization of software-based implementations that use data array copies.

Cascading updates: Since proxy ownership within each region is allocated in the same way, the proxy tiles for a particular array element are on the same row/column for horizontally/vertically aligned proxy regions. Therefore, as a task invocation travels towards the owner tile across the NoC, it will naturally pass by its corresponding proxy tiles en route (Fig.2, blue arrows). The router of a proxy tile has the option to grab a proxy task if the tile is free and there is NoC contention on the port towards the owner tile. This alleviates NoC traffic and increases load-sharing. We call this *selective cascading*. Proxy tiles closer to the owner tile are more likely to have the most updated value, leading to the filtering of unnecessary updates in a cascading manner.

Takeaway 1. Proxy regions and selective cascading provide the following advantages: (a) *smooth out work imbalance* by allowing multiple tiles to operate on a given data; and (b) *minimize the # of bytes traversing the NoC* by coalescing updates to the original data array en route; (c) *reduce NoC contention* by opportunistically deciding whether proxy tasks are executed at proxy tiles, or they continue towards the owner.

3.2. Software-configurable Queues and NoC

Task Scheduling and Queue Sizes: To mitigate back-pressure from end-point routers, input queues must have a sufficient size to buffer message bursts. These bursts naturally happen when a column of a sparse matrix is much denser than the rest. Conversely, making queues too large can cause messages to wait too long on average to be processed, leading to data staleness. Since there is no global orchestration of tasks, scheduling solely depends on information that is local at each tile. Thus, queue occupancy and back-pressure help signal tiles to adapt their task scheduling to prioritize tasks leading to higher overall utilization, effectively resulting in a Goldilocks effect. Tascade queue sizes are configurable in software. We study the performance impact of queue sizes in §5.2. We observe that optimal queue sizes are application-specific, which is related to applications’ sensitivity to data staleness. We envision that workload- and task-specific queue sizes can be set by a compiler via static analysis and the communication

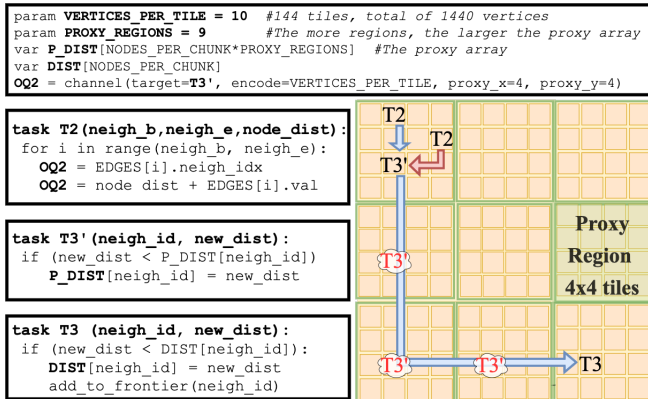


Figure 2: Software configuration of proxy regions and flow of tasks for single-source shortest path (SSSP). This grid example configured 9 proxy regions of 4x4 tiles. Each region contains proxy owners for an entire data array (P_DIST), where each tile *is a proxy for* a fraction of it. Contrary to Dalorex, in Tascade, T2 invokes T3', which targets a proxy tile within the same region. T3' tasks write to P_DIST, which lives in the proxy cache (P\$, see §3.3). The blue arrow shows a T3' that results in an eviction in P\$ and triggers a T3 invocation to the data owner. The red arrow shows a T3' that does not result in an update in P\$. Through selective cascading, en route to the owner, this message can also invoke T3' at a local proxy indicated by clouds when there is NoC contention.

distance between tasks. This can also help utilize the storage better and give more SRAM to the caches (§3.3).

NoC-to-task Mapping: In a Tascade system, there are P physical NoCs and C logical channels. These channels can be assigned to different physical NoCs or the same one. If they are in separate NoCs, these messages are routed uncontested. If they are in the same NoC, they are arbitrated in a round-robin fashion. The allocation of physical to logical resources is fully reconfigurable, a NoC can be used by multiple tasks, and a task can use multiple NoCs. If an application is not using all of the available NoCs, a task can use more than one channel to increase the bandwidth for this task.

Takeaway 2. Software-configurable queues enable selecting a sufficient size that helps maintain a software pipeline effect in this task-based throughput-oriented architecture while minimizing the SRAM resources utilized for that. The software mapping of task channels to physical NoCs enables optimally allocating network resources given the consumption and production rate of certain task types.

3.3. Software-configurable Caches

Tascade designs the SRAM in each tile such that it can be used either as a scratchpad or as a cache [40, 15, 16]. The cache mode stores cacheline tags in SRAM, including a valid bit. To minimize the hardware and energy overhead of using the SRAM as a cache, we make the caches directly mapped.

This cache mode is used to configure the *proxy cache* (P\$), which holds proxy data, and the *data cache* (D\$), which holds original (exclusive owner) data arrays. When scaling out the

Tapeout-time Design Decisions

- # of Tiles per die
- SRAM per-tile (MiB)
- #Physical NoCs and Width of each one (in bytes)
- Max.# of Router Buffer Entries per Physical NoC
- Max.# of Logical NoC Channels per Physical NoC
- Max.# of Memory Controller Channels per TCA die

Packaging-time Design Decisions

- # of TCA dies per package
- # of DRAM dies per package and capacity of each (GiB)
- TCA-DRAM ratio dictates Mem. BW and Capacity per TCA die
- # of I/O dies per package (Off-Package BW)

Compile Time Configurations

- Size and Place of the grid that the workload uses (grid of dies)
- Whether the dataset uses SRAM as a scratchpad or D\$
- Size of the D\$ (in data elements)
- Mapping of Tasks to Logical NoC Channels
- Mapping of NoC Channels to Physical NoCs
- # of Router Buffer Entries of each NoC Channel (shared pool)
- Arbitration ratio between Channels sharing a Physical NoC

Per Task

- If a Task has a Proxy and the size of the Proxy region
- If the Proxy array is cached or kept in full
- If a Task uses data prefetching during execution (if cached dataset)
- Input Queue (IQ) Size
- Output Queue (OQ) Size if the Task produces into a NoC Channel

Table 2: Reconfigurable Parameters of Tascade

parallelization of a dataset, if the memory footprint per tile is low-enough to fit in the local SRAM, the D\$ would not be configured, the PUs would access the data arrays as a scratchpad, and the memory controller and the HBM would be switched off. The footprint of a P\$ decreases when the size of the proxy region increases (the performance impact of region sizes is studied in Fig. 7). The D\$ and the P\$ have reconfigurable sizes. When multiple tasks use proxies, each task would configure its own logical P\$, although they all use the same comparison logic. Only one D\$ can be configured, and its line width equals the bitline width of the DRAM memory controller (512 bits in our experiments with HBM).

D\$ misses and evictions: Upon a miss, the D\$ fetches the full cacheline from DRAM without checking for coherence since the data is not shared. Each tile's local SRAM is backed up by a DRAM storage of size $DRAM_capacity/tiles_per_die$. (The details of the DRAM devices assumed for the evaluation are described in Table 3.) The D\$ has one dirty bit per line to write back to DRAM upon eviction. Since the D\$ of each tile only contains the part of the dataset that the tile is responsible for, there are no coherence issues for modified data.

P\$ misses and evictions: A miss in the P\$ returns a default predefined value such as 0 for Histogram or infinite for SSSP.

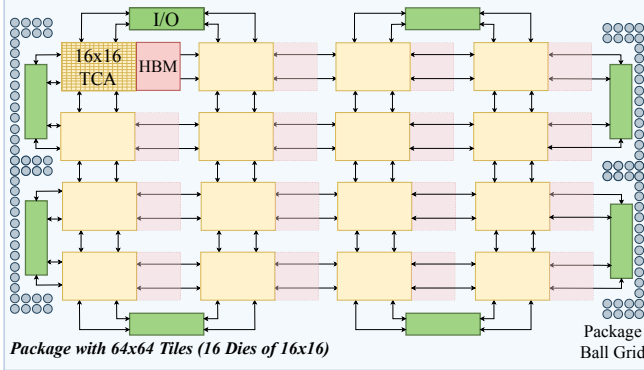


Figure 3: Top view of an example chip package with 64x64 tiles. The number of TCA dies would determine the compute capacity, while including HBM dies would determine the compute-to-memory ratio of the chip architecture. The number of I/O dies (and their resources) would determine the provisioned off-chip bandwidth.

On eviction, the data is simply replaced in a write-back manner, and so the evicted data is sent as a task targeted to the data owner. In our experiments, a P\$ line contains one element to avoid sending multiple updates upon eviction.

Prefetching: The PU has a very simple in-order pipeline, which stalls waiting for data on a D\$ miss. Since the first parameter of every task message contains an array index, and the TSU knows to which array it corresponds (used for NoC routing), we use this information to prefetch the data. A task may access more than one array using the same index, so we add another pointer to the TSU’s per-task table so that it prefetches both when needed. Those tables also have an extra bit saying whether the PU keeps prefetching data during the task execution. Since pointer indirections are split into tasks, when tasks access multiple array elements, they often do it with a streaming pattern. To prefetch these, we enable PU’s next-line prefetcher for tasks that access multiple elements.

Takeaway 3. Software-configurable caches enable utilizing the SRAM efficiently by balancing the resources dedicated to D\$ and P\$, depending on what is their footprint. E.g., when sharding a dataset across more tiles, its footprint per tile decreases, and more SRAM can be dedicated to P\$.

3.4. Packaging-time configurability

Memory technology and integration: The memory hierarchy determines the bandwidth available to computing units and, thus, at which level of arithmetic intensity the chip becomes memory-bound. To increase memory bandwidth, prior work has proposed having DRAM on the chip. Some proposals assumed 3D integrations where processing cores are on the base plane of the 3D-stacked memory, accessing the TSVs directly [4, 92, 93, 38]. However, this may render impractical. There are very few foundries that can fabricate HBM technology, and the design seems to only change with every generation of JEDEC specification [32] (e.g., HBM2, HBM2e, HBM3) which vendors conform to. So it would be expensive to fab-

ricate an HBM die with a custom base layer. Moreover, the base layer of the HBM stacks is filled with MBIST logic and PHY [44, 68, 30, 59]. Alternatively, other works have proposed integrations of off-the-shelf HBM dies with compute dies by having the compute dies surrounded by HBM devices on the edges of the chip [55, 5, 49, 31, 56, 91, 88, 14]. Tascade is the first proposal for having horizontally-integrated HBM dies interleaved across columns of compute dies. This allows the design of TCA dies to be agnostic to the # of TCA and DRAM dies that are eventually integrated on-chip.

Interleaving DRAM & TCA dies: Figs. 1 and 3 depict the integration of TCA, and HBM dies via a passive silicon interposer. This provides higher TCA-HBM bandwidth than a silicon bridge [49] or substrate integration [41, 5]. The interposer only contains the wires between a TCA die, and its HBM die since HBM access is exclusive. The links connecting TCA dies are routed through the organic substrate, which also contains the power delivery and redistribution layer (RDL).

How much DRAM can be included? HBM capacity can be increased by either stacking more DRAM layers or having larger layers. In our evaluation, we assumed a 10x11mm 4-layer HBM die (up to 16 layers have been demonstrated [68]). One could also integrate larger HBM dies, provided that the distance between TCA dies remain within 25mm (limit of common PHYs for MCM [76, 60, 6]).

How much DRAM should be included? In addition to the arithmetic intensity of the target application, selecting the amount of DRAM on the chip depends on the expected level of parallelism for the final product. If the chip is always expected to parallelize a dataset to the limit of strong scaling (having little workload per tile), HBM might not be necessary. In contrast, with target metrics like performance-per-watt, larger on-package memory capacity is essential. We evaluate both options in §5.4 and discuss the tradeoffs.

Memory controller: As depicted in Fig. 1, the memory controller lives on the TCA die, and thus, in case of not integrating DRAM, it becomes *dark silicon*. Although in our evaluation, we consider it as such, an idea for a future design would be to have an embedded FPGA logic that allows hardening a memory controller or other computing logic (in the case DRAM is not integrated). Another advantage is enabling a DRAM technology like DDR (which may use a different memory controller than HBM) to tradeoff capacity for bandwidth.

Designing the NoC: When dealing with irregular traffic in dimension-ordered routing (DOR), a 2D torus provides a more uniform utilization than a 2D mesh [63]. DOR keeps the router logic simple, and deadlocks are avoided using bubble routing [73]. To make implementation practical on 2D silicon, the 2D torus is folded: one set of links connects the even-numbered tiles, and the other set of links connects the odd-numbered ones. The torus can be arbitrarily large, i.e., be confined within a die or span multiple dies, packages, or boards. Table 3 presents the interconnect energy and latency assumed for our evaluation at each level. Fig. 4 shows that the

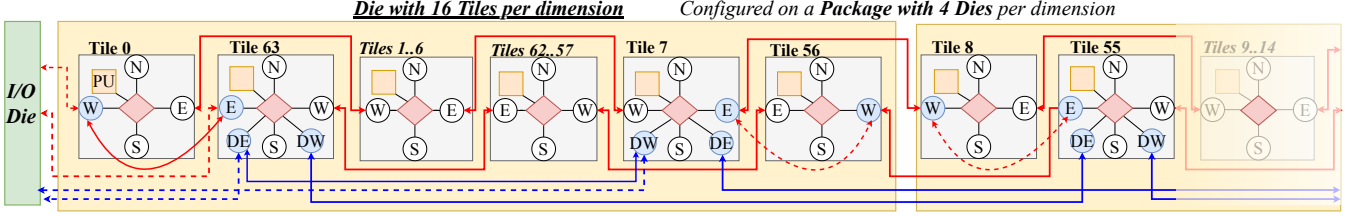


Figure 4: Horizontal links within a TCA die and across dies. The red links show the NoC that connects every tile (*tile-NoC*), while the blue links show the NoC that connects to one tile per die (*die-NoC*). Because of the die-NoC, the routers at the die edges are radix-9, while the rest are radix-5. The ports shadowed in blue are runtime reconfigurable; any tile subgrid within the system may become torus (including across packages). The dies on the edges of a package will interface with the I/O die. All I/O links are configured when loading the dataset to maximize I/O bandwidth. During program execution, both NoCs may become torus, or tile-NoC torus, and die-NoC mesh, to keep streaming from I/O.

routers at the edges of each die can be configured to connect to a router on the next die or wrap around by connecting to the adjacent tile (Tiles 0 and 63).

Reconfigurable topology: We can reconfigure a 2D-torus NoC into two 2D-mesh NoCs by not connecting the wrap-around links on the routers at the edges. Utilizing two mesh NoCs may be the right choice when running a workload with near-neighbor communication [7]. As Fig.4 shows, Tascade has two hierarchical NoCs, one that connects every tile and one that hops once per die. Each NoC topology is individually configured. While bringing the data inside the package from disk, they both would be configured as a mesh to enable data streaming from the I/O dies. During the execution, both may become torus, or the die-NoC can remain open to I/O data.

Off-Chip Bandwidth: Our design uses I/O chiplets to connect chip packages. This allows TCA dies to remain agnostic to a specific off-chip protocol (e.g., PCIe 6.0 [75]). It also defers choices like off-chip bandwidth to packaging time, so they are taken based on the requirements of the final product. The off-chip bandwidth could be as high as the I/O-TCA bandwidth.

What decides the package size? A package is as big as the size of its substrate. A silicon substrate typically scales 2-3x the reticle size, but this could technically scale up to a wafer-scale interposer [67]. On a Multi-chip Module (MCM) integration, server-class chip packages typically span over $4500mm^2$ [55, 5, 56]. However, MCM substrates have been fabricated to nearly $100,000mm^2$ [84, 22]. So the choice of the package size may be determined by the unit of sale rather than a constraint in the substrate size. Regarding the number of dies on a package, although we see chip packages with tens of them [26], bonding may set feasibility bound. The bonding yield of each die determines the overall package yield. [85]. When using Tascade dies of 16×16 tiles, the practical limit may be 128×128 tiles per package (64 dies). In our evaluation, we use a chip containing 64×64 tiles (shown in Fig. 3); it spans $4780mm^2$, which is in line with the size of server-class chips.

Scaling beyond a package: Off-chip interconnect topology and bandwidth are determined by the I/O chiplets selected. The I/O links across packages could also be electrical or optical [51, 19]. If a system featuring TCA chiplets is expected

to have near-neighbor communication, several packages can simply be connected on a board using a 2D interconnect with electrical links. However, when irregular or all-to-all traffic is expected, it would be beneficial to connect packages with optical links on a low-diameter interconnect [9, 3, 10]. Despite our evaluated workloads being irregular, for simplicity, we assumed a 2D network with electrical links across packages.

Data partitioning is a preprocessing step used in distributed graph processing to minimize cross-node communication [86, 36]. In addition to proxies, Tascade could potentially use partitioning and place the data so that each subgrid holds a partition. However, our evaluation did not need to resort to it.

Takeaway 4. Tascade proposes a chiplet-based architecture that allows making key design decisions, such as on-chip memory and off-chip interconnect, post-silicon. This enables the same TCA design to be mass-produced (saving NRE costs) and later integrated differently to create products with varying target metrics. We have discussed cases that benefit from one configuration or another—some of which are evaluated in §5.

4. Evaluation Methodology

Applications: We evaluate the performance of Tascade on four graph workloads, one sparse linear algebra, and a histogram benchmark [81] to demonstrate the generality of our approach for memory-intensive applications. *Breadth-First Search (BFS)* determines the number of hops from a root vertex to all vertices reachable from it; *Single-Source Shortest Path (SSSP)* finds the shortest path from the root to each reachable vertex; *PageRank* ranks websites based on the potential flow of users to each page [42]; *Weakly Connected Components (WCC)* finds and labels each set of vertices reachable from one to all others in at least one direction (using graph coloring [78]); *Sparse Matrix-Vector Multiplication (SPMV)* multiplies a sparse matrix with a dense vector. *Histogram* counts the # of values that fall within a series of intervals.

Datasets: We use various sizes of the RMAT [45] graphs—standard on the Graph500 list [54]—e.g., RMAT-26 (abbreviated as R26 in §5) contains 2^{26} vertices (V) and 1.3B edges (E), and has a memory footprint of 12GB. We also use the Wikipedia (WK) graph (V=4.2M, E=101M) in our evaluation.

Simulation: Our evaluation uses muchiSim [64], the cycle-

Memory Model Parameters	Values
SRAM Density	3.5 MiB/mm ² [89]
SRAM R/W Latency & E.	0.82ns & 0.18 / 0.28 pJ/bit [89]
Cache Tag Read & cmp. E.	6.3 pJ [89, 90]
HBM2E 4-high Density	8GiB/110mm ² (75 MiB/mm ²) [44]
Mem.Channels & Bandwidth	8 x 64 GB/s [44]
Mem.Ctrl-to-HBM RW Latency & E.	50ns & 3.7pJ/bit [66, 37]
Bitline Refresh Period & E.	32ms & 0.22pJ/bit [79, 24]
Wire & Link Model Parameters	Values
MCM PHY Areal Density	690 Gbits/mm ² [6]
MCM PHY Beachfront Density	880 Gbits/mm [6]
Si. Interposer PHY Areal Density	1070 Gbits/mm ² [6]
Si. Interposer PHY Beachfront Density	1780 Gbits/mm [6]
Die-to-Die Link Latency & E.	4ns & 0.55pJ/bit (<25mm) [60]
NoC Wire Latency & E.	50 ps/mm & 0.15pJ/bit/mm [38]
NoC Router Latency & E.	500ps & 0.1pJ/bit
I/O Die RX-TX Latency	20ns [75]
Off-Package Link E.	1.17pJ/bit (80mm) [88]

Table 3: Energy (E), bandwidth, latency, and area of links and memory devices assumed for the evaluation.

level manycore simulator that was used to evaluate prior work Dalorex [63]. We extended muchiSim to support chiplets and on-chip DRAM; Table 3 summarizes our additions to the energy, latency, and area model for communication links and memory technology. We assume the same logic frequency as Dalorex, 1GHz. We also added a cost model to study the cost-effectiveness of different Tascade configurations.

Cost Model: For *silicon*, we assume that a 300mm wafer with a 7nm transistor process costs \$6,047 [34]. We obtain the cost per die by dividing the wafer cost by the number of good dies per wafer (calculated using Murphy’s model [53] with 0.2mm scribes, 4mm edge loss, and 0.07 defects per mm^2). When comparing cost-effectiveness in Fig.9, we do not include the Non-Recurring Engineering (NRE) cost of the TCA dies since all the options use the same TCA chiplets. In terms of *packaging*, all our results featuring grid sizes over 64x64 use multiple packages (of 64x64 tiles each, based on our rationale from §3.4). We assume the cost of the 65nm silicon interposer connecting a TCA die with HBM (including bonding) to be 20% of the price of a TCA die [85]; the cost of an organic substrate to be 10% of the price of an equal-sized TCA die, and the bonding to add an additional 5% overhead [80, 43]. Regarding *DRAM*, we assume an 8GB HBM2E device with eight 64GB/s memory channels. While this cost is not disclosed, we made an educated guess using public sources [34, 69]. We assume 7.5\$/GB, which is more affordable than when HBM was released in 2017. One could expect this price to decrease over time as more vendors fabricate HBM [52, 44, 59].

Graph500 methodology: To understand where our system stands on the Graph500 list [54], we follow their guidelines. They measure separately reading and preparing the graph from the search itself. We do not perform any dataset pre-processing

and directly read the CSR structure from the disk. Since our goal is to evaluate the performance of our architecture, we focus on the graph search time. We begin counting cycles when the search key is loaded onto the system and stop counting when the last vertex is visited. We perform one search and report traversed edges per second as $TEPS = m/time$ where m is the number of edges connected to the vertices in the graph traversal starting from the search key. Since we also evaluate other workloads than graphs, when we report TEPS for SPMV and Histogram, we consider the number of dataset elements.

5. Results

This section starts by characterizing Tascade’s settings, which are—as shown in Table 2—configurable at various levels. Particularly, §5.1 is about pre-silicon choices: it shows the **performance impact** of four NoC options and discusses tradeoffs for **SRAM capacity** per tile and **die size**. §5.2 characterizes the impact of the software-configurable **queue** sizes in application runtime and PU utilization. §5.3 presents the performance gained from using **proxy** regions over prior work Dalorex and analyzes different region sizes. §5.4 studies the **cost-effectiveness of integrating HBM dies** in terms of performance and energy efficiency per dollar. Finally, §5.5 studies strong scaling (by parallelizing R26 for grid sizes ranging from 256 tiles to 1,048,576 tiles) and presents performance-per-watt and per-dollar results. §5.5 also compares our BFS results with the most performant entries of the Graph500 list [54] and other works [11] for two datasets sizes.

5.1. Pre-silicon Choices

SRAM size: We simulated with SRAM sizes ranging from 128KiB to 4MiB and found 1.5MiB per tile to suffice to hold the program code, task queues, and a performing size of D\$ and P\$. The P\$ saves intra- and inter-die traffic on the task for which it is enabled, reducing the task’s average number of router hops. The ideal size of the P\$ depends on the ratio of the size of the grid (in which a program is running) and the proxy grid. The D\$ saves traffic to the HBM device, reducing memory-controller contention and energy. An appropriate size of D\$ yields a hit rate that is high enough not to saturate the memory channels when the processing units are fully utilized. Cache sizes are compile-time configurable, as mentioned in §3.2. At 1.5MiB, the tile area dedicated to SRAM is 7× larger than the area of the router, PU and TSU together. Since Tascade is data-centric, this size is a good tradeoff.

Die size: Our evaluation uses chiplets of 16x16 tiles. This die size is practical because: (a) it matches common sizes of HBM chiplets [44, 68, 59]; (b) it allows for larger configurations per package, as the packaging yield depends on the number of dies; (c) the lower yield of a 32x32-tile die (27x25mm) results in 62% less good dies per wafer [53]. Although prior work used large dies with high yield at the expense of adding tile redundancy [47, 39], we find it appealing to have a unit die that is small enough to add flexibility at packaging time.

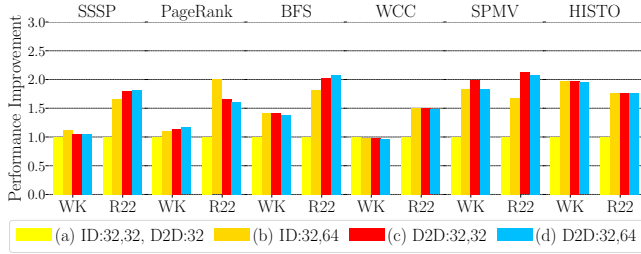


Figure 5: Performance improvement of increasing link widths over a baseline of two 32-bit NoCs intra-die (ID) throttled to a shared 32-bit die-to-die (D2D) link.

Studying NoC width: Fig.4 showed that Tascade uses a die-NoC that hops between dies and a tile-NoC that hops logically adjacent tiles. We use a single 32-bit die-NoC for all our evaluations. We characterize how the number and width of the intra-die (ID) and die-to-die (D2D) links of the tile-NoC affect runtime in Fig.5, including: (a) two 32-bit links (i.e., two NoCs) whose flow gets throttled to a shared 32-bit link when crossing die boundaries; (b) a 32-bit and a 64-bit link, also throttled to a shared 32-bit link when crossing die boundaries; (c) same as b but with two 32-bit links across dies; (d) 32-bit and 64-bit links, both inside and between dies. We map the channels that deliver the most frequent task type and its proxy (e.g., T3 and T3' in Fig.2) into the 64-bit NoC (if any), while other tasks use the 32-bit NoC.

NoC tradeoff: Fig.5 shows that across the board, the geometric improvement of option c with two 32-bit links across dies is 51% geometrically faster than option a. Since the NoC width is determined pre-silicon, it is essential to understand its tradeoffs. The die area of c grows by 4.5% over that of a, but the performance improvement renders it worth it.¹

Choices for the rest of the evaluation: All other experiments in §5 use option c. Note that the characterizations shown in Figs.5,6,7 evaluate using a 64×64 tile grid that fits within a single chip package of 16 dies (as in Fig.3). All but Fig.7 results use proxy regions of 16x16 tiles, matching the die size. Thus, there are 16 regions overall in the 64×64 grid.

5.2. Queue Size Effects on Performance

Fig.6 (top) shows the performance gained from increasing the size of IQs (while OQ size is kept constant). There are tradeoffs associated with queue sizes. Small IQ sizes lead to end-point contention as message bursts arrive, and the PU is unable to process them quickly enough. Large IQ sizes contribute to increased data staleness and work redundancy in graph applications and also consume SRAM resources that could be dedicated to caches. Fig.6 shows a peak in the perfor-

¹The interconnect between TCA dies in c is right below the limit of what is supported with MCM (~800Gbit/s/mm) to avoid a more expensive interposer needed for (d) that can reach up to 5Tbit/s/mm [88, 60, 76]. For the die-to-die substrate wires, we assume BoW-128 PHYs with 130μm bumps [60, 6]. To connect TCA and HBM, we assume a 65nm CMOS passive interposer [72, 13] with 55μm bumps [60].

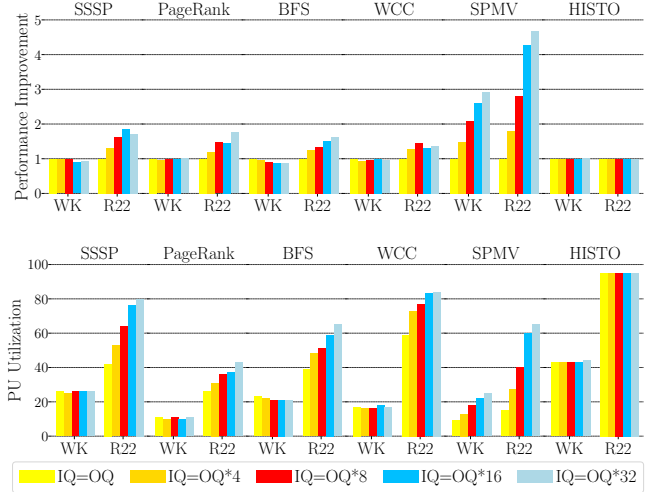


Figure 6: Increase in performance (top) and % PU utilization (bottom) when growing the input queue (IQ) size—keeping the same output queue (OQ)—normalized to a baseline of equal IQ and OQ size.

mance of SSSP, BFS, and WCC for smaller queue sizes—as they are most sensitive to staleness—whereas the performance for SPMV improves as the IQ size increases. The absence of general improvement for WCC and Histogram on K22 can be attributed to the already-high core utilization we observe for these workloads.

Regarding the utilization shown in Fig.6 (bottom), note that the footprint per tile is only 2^{10} vertices for R22 executed on 2^{12} tiles and only half as many for Wikipedia dataset. Achieving 100% utilization is challenging at this extreme level of parallelization because the cool-down phase (during which there is a long tail of a few PUs executing the final tasks) represents a significant portion of the total runtime.

All other experiments in §5 employ an IQ-OQ ratio of 16.

5.3. Proxy Regions Improve Performance and Scalability

Fig.7 displays the performance impact of various sizes of proxy regions over a baseline of not using proxies. This no-proxy setup serves as our method for evaluating Dalorex, as we aim to measure the performance improvements stemming from the proxy regions without considering specific physical implementation design choices.

Proxy advantages: Tascade is geometrically 2.6× faster than Dalorex (up to 4.4×) across datasets and apps. As §5.4 will show, using proxy regions also improves energy efficiency since updates get coalesced at proxy tiles, and fewer bytes travel all the way towards the data owner.

Scalability: Fig.8 presents our evaluation of Tascade—using proxies of 16x16—and Dalorex on three strong-scaling steps for each dataset, ranging from 64x64 to 256x256 for R25 and from 128x128 to 512x512 for R26. Note that the starting point is not arbitrary; it is the minimum grid size in Dalorex that can hold the entire dataset on SRAM. In contrast, Tascade can integrate HBM during packaging, and thus, it can run

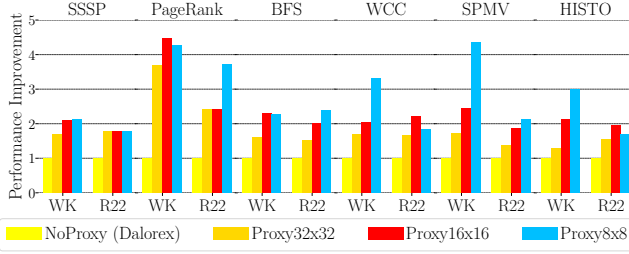


Figure 7: Performance gain with decreasing sizes of proxy regions normalized to the baseline of no proxy,

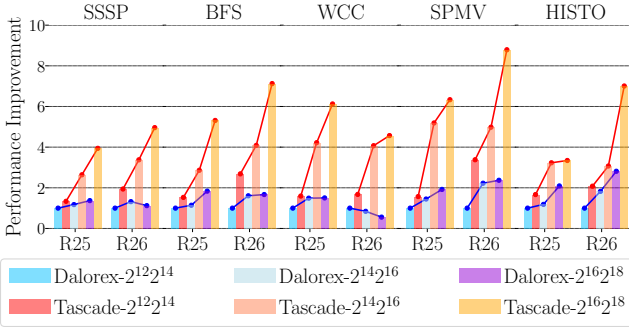


Figure 8: Performance gain of three scaling steps for each dataset. R25 uses a 64x64 (2^{12} tiles), 128x128 (2^{14}) and 256x256 (2^{16}) grid for these strong scaling steps, while R26 uses 128x128 (2^{14}), 256x256 (2^{16}) and 512x512 (2^{18}).

large datasets starting from smaller grids, as we evaluate on §5.5. However, Fig.8 compares Dalorex and Tascade using the same grid sizes and no HBM. Dalorex starts to plateau after 64x64 due to high NoC contention, while Tascade continues to scale. For the last scaling step, Tascade is on geomean 3.3× faster than Dalorex across datasets and applications. Tascade achieves a speedup of 5.8× over the first scaling step (and up to 8.8× for SPMV on R26), while Dalorex only achieves 1.75× speedup.

5.4. Package Integration Alternatives

We evaluated throughput and energy efficiency per unit of cost of two Tascade integrations over Dalorex (Fig.9). As advanced in Fig.1, the Tascade integrations we study are (a) having only TCA dies (and so all memory is on SRAM), and (b) having HBM devices interleaved horizontally between TCA dies, via a passive interposer. Since the silicon area of a 64x64 configuration of Dalorex [63] is beyond the reticle limit of 880mm², we assume the same chiplet-based integration for Dalorex, as we have done in the previous section. This makes their cost very similar (only affected by the interconnect area). Thus, throughput-per-cost differences mostly come from the runtime. We evaluate all integrations on their smallest configuration that fits the dataset. This makes the HBM integration use a tile grid of 16 times fewer tiles.

Although Fig.9 does not show absolute throughput, we can observe from Fig.11 (also using R26) that it scales. Since

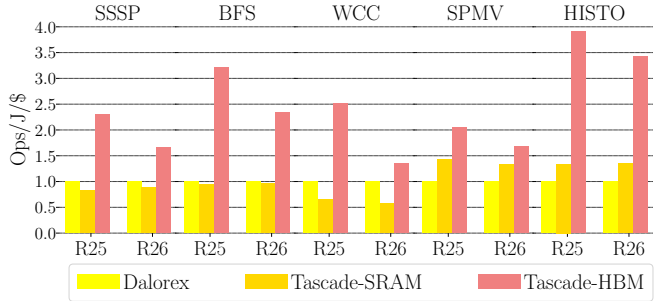
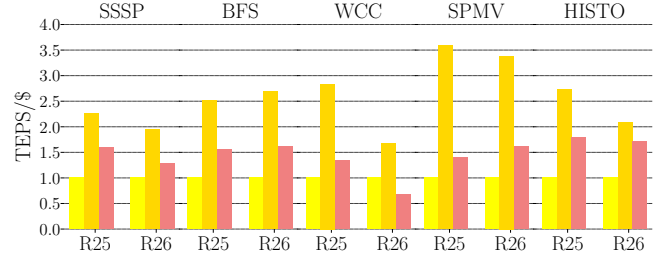


Figure 9: Normalized improvements in throughput/\$ and energy efficiency/\$. Dalorex and Tascade-SRAM run on 64x64 tiles (16 dies of 16x16) for R25 and 128x128 for R26, while Tascade-HBM uses 16x16 tiles for R25, and 32x32 for R26.

the SRAM configuration of Tascade does not cost 16× more than the one including HBM, Tascade-SRAM wins across the board on throughput-per-dollar. However, Tascade-HBM wins on energy-efficiency-per-dollar. This throughput-per-dollar results could change significantly if either HBM becomes cheaper (currently 3× more expensive than the TCA die) or another DRAM or 3D-stacked SRAM [77] technology becomes cheaper.

We show the breaks down of the energy used by PUs, memory, and NoC for Tascade-SRAM and Tascade-HBM in Fig.10. Since the SRAM-only integration scales out to use 16× more tiles than Tascade-HBM, it spends more energy on wires. Although not shown here, we observed that the HBM integration saturates the memory controller bandwidth. This makes the energy usage dominated by DRAM; PUs use a small fraction in both cases. Note that PUs are powered off when idle, so they only consume energy while processing tasks.

5.5. Strong Scaling Up to a Million Tiles

Throughput-per-watt likes small grids: Fig.11 (bottom, red bars) shows that if throughput-per-watt is the target metric, staying within the smallest configuration that fits the dataset is the correct choice. The R26 dataset fits entirely on a 16x16 die with 8GB HBM. Throughput-per-watt drops significantly after using 2^{12} tiles, i.e., a chip package of 64x64 tiles. The inter-package links are more power-hungry than the ones inside the package, hence, the drop in efficiency.

Throughput-per-dollar increases during superlinear performance scaling: While the cost grows linearly with the number of chips, the performance grows super-linearly un-

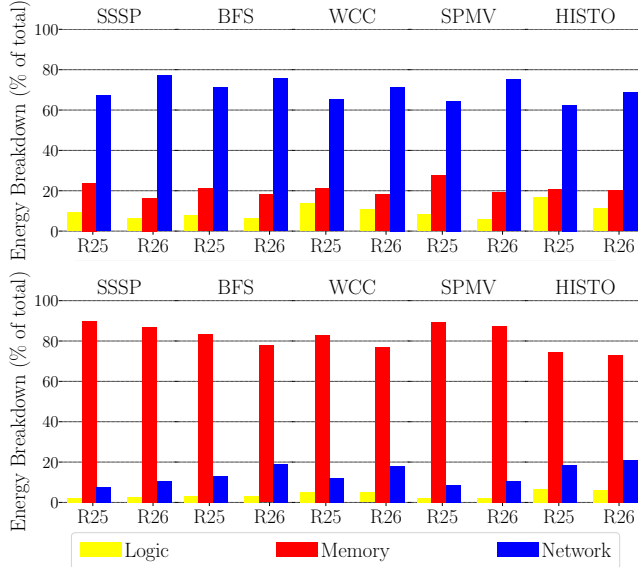


Figure 10: Breakdown of the energy consumed by computing logic, memory, and NoC communication (including routing and wire energy), for Fig.9’s Tascade-SRAM (top) and Tascade-HBM (bottom). The Y-axis shows the % of the total energy spent on each component.

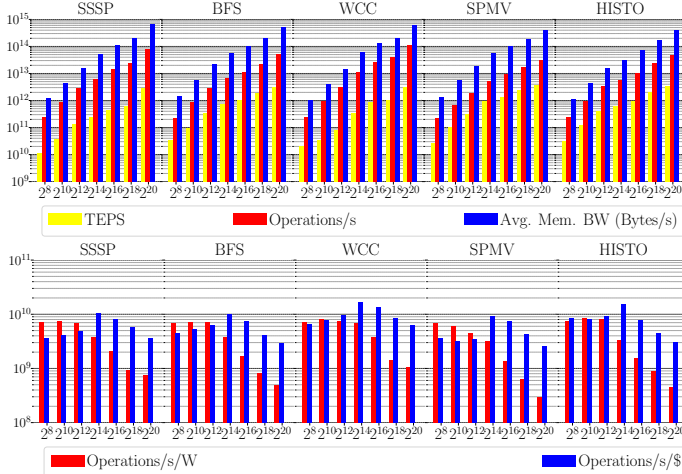


Figure 11: Throughput in operations, traversed edges per second (TEPS), and the average on-chip memory bandwidth needed to achieve that. The X-axis is the size of the Tascade grid used when analyzing strong scaling R26, ranging from 256 to over a million tiles. The bottom plot shows throughput as a function of power and cost. Higher is better.

til the scaling step, where the decrease in footprint-per-tile also decreases the pressure in the memory controller of the HBM. As a result, we observe that the optimal throughput-per-dollar peaks at a 128x128 configuration (4 chip packages) (Fig.11 bottom, blue bars). At 128x128, R26 fits in SRAM, and any smaller footprint-per-tile reduces PU utilization since there are fewer parallel tasks to be executed. This leads to the throughput-per-dollar to decrease beyond this point.

Strong scaling for faster time-to-solution: For purposes of this experiment, we take the extreme approach of parallelizing a dataset with 2^{26} vertices (and $\sim 2^{28}$ edges) across 2^{20} tiles. This shows that Tascade is suited for strong scaling, although it is not the most efficient way to use it.

Petabyte/s of memory bandwidth: As mentioned earlier, data-structure traversal has a high memory-to-compute ratio. Fig.11 demonstrates how much memory bandwidth is required to maintain a high target throughput. For the 1-million-tile configuration, SPMV reads, on average, almost half a PB/s from their local memories. At peak, SPMV reads 2.2 PB/s to perform 415 Teraops/s, of which 41 Teraops/s are dedicated to the multiplication of non-zero matrix elements. This configuration uses 256 chip packages and draws 12KW of power on average and 40KW at its peak— power density stays within the tens of mW/mm² suitable for air cooling.

Comparing with the state-of-the-art: Top two performances for BFS on R26 in Graph500 list are Tianhe Exa-node (Prototype@GraphV) [54] and an undisclosed *High Throughput Computer* with four NVidia V100-SXM2, delivering 884 and 392 GTEPS, respectively. For R26, our work performs 1826 GTEPS on a 512x512 grid (128 chips) and 3021 GTEPS on a 1024x1024 grid (256 chips). Bringing the dataset onto the chip would take < 0.1 ms, given the assumed chip I/O and the number of chips. For smaller datasets like R22, best performing prior work is unlisted on Graph500 and demonstrates up to 70 GTEPS [11] running the Enterprise [48] and Gunrock codes [87] on a 32GB NVIDIA Tesla V100-SXM3. For R22, the 64x64 configuration (single-chip) evaluated in Fig.6 achieves 362 GTEPS (5.2 \times improvement). Note that this GPU runs at 1.6 GHz, while our system assumes 1 Ghz.

6. Conclusion

This paper demonstrates that Tascade scales performance for sparse-data applications even when parallelized to an unprecedented degree, such as processing 2^{26} vertices across 2^{20} PUs. This degree of parallelization is 100 \times greater than the previous largest one for this problem size. Moreover, our BFS throughput is higher than the top entries of the Graph500 list.

We achieve this by introducing proxy regions and selective cascading. Our proxy approach mitigates the work imbalance arising from the massive parallelization of sparse datasets by allowing proxy tiles to perform tasks (using copies of the data) on behalf of the data owner. Data updates are propagated seamlessly and opportunistically (improving NoC utilization) thanks to the write-back proxy caches and selective cascading.

We put much effort into making a chiplet-based design that is highly configurable, not only so that it could potentially be applied to other domains, but also within the same domain, to optimize the chip at packaging time for different target metrics. Our evaluation shows that packaging the same TCA chiplets with or without on-chip DRAM leads to different throughput and energy-efficiency per-dollar results and different optimal scaling steps for throughput-per-watt.

References

- [1] Sriram Ananthakrishnan, Nesreen K Ahmed, Vincent Cave, Marcelo Cintra, Yigit Demir, Kristof Du Bois, Stijn Eyerman, Joshua B Fryman, Ivan Ganev, Wim Heirman, et al. Piuma: programmable integrated unified memory architecture. *arXiv preprint arXiv:2010.06277*, 2020.
- [2] Maleen Abeydeera and Daniel Sanchez. Chronos: Efficient speculative parallelism for accelerators. In *Proceedings of the Twenty-Fifth International Conference on Architectural Support for Programming Languages and Operating Systems*, pages 1247–1262, 2020.
- [3] Narasimha R Adiga, George Almási, George S Almasi, Yariv Aridor, Rajkishore Barik, D Beece, Ralph Bellofatto, Gyan Bhanot, Randy Bickford, M Blumrich, et al. An overview of the bluegene/l supercomputer. In *SC'02: ACM/IEEE Conference on Supercomputing*, pages 60–60. IEEE, 2002.
- [4] Junwhan Ahn, Sungpack Hong, Sungjoo Yoo, Onur Mutlu, and Kiyoung Choi. A scalable processing-in-memory accelerator for parallel graph processing. In *Proceedings of the 42nd Annual International Symposium on Computer Architecture*, pages 105–117, 2015.
- [5] AMD. AMD rome, 2018. <https://en.wikichip.org/wiki/amd/cores/rome>.
- [6] Shahab Ardalan, Bapi Vinnikota, Tawfik Arabi, and Elad Alon. What is the right die-to-die interface? a comparison study, 2022. <https://www.opencompute.org/events/past-events/hipchips-chiplet-workshop-isca-conference>.
- [7] Krste Asanovic, Ras Bodik, Bryan Christopher Catanzaro, Joseph James Gebis, Parry Husbands, Kurt Keutzer, David A Patterson, William Lester Plishker, John Shalf, Samuel Webb Williams, et al. The landscape of parallel computing research: A view from berkeley. *eScholarship, University of California*, 2006.
- [8] Jonathan Balkind, Katie Lim, Fei Gao, Jinzheng Tu, David Wentzlaff, Michael Schaffner, Florian Zaruba, and Luca Benini. OpenPiton+Ariane: The first open-source, SMP Linux-booting RISC-V system scaling from one to many cores. In *Third Workshop on Computer Architecture Research with RISC-V, CARRV*, volume 19, 2019.
- [9] Alan Benner. Optical interconnect opportunities in supercomputers and high end computing. In *OFC/NFOEC*, pages 1–60. IEEE, 2012.
- [10] Maciej Besta and Torsten Hoefler. Slim fly: A cost effective low-diameter network topology. In *SC'14: proceedings of the international conference for high performance computing, networking, storage and analysis*, pages 348–359. IEEE, 2014.
- [11] Luk Burchard, Johannes Moe, Daniel Thilo Schroeder, Konstantin Pogorelov, and Johannes Langguth. ipug: Accelerating breadth-first graph traversals using manycore graphcore ipus. In *International Conference on High Performance Computing*, pages 291–309. Springer, 2021.
- [12] Cerebras Systems Inc. The second generation wafer scale engine. <https://cerebras.net/wp-content/uploads/2021/04/Cerebras-CS-2-Whitepaper.pdf>.
- [13] Raghunandan Chaware, Kumar Nagarajan, and Suresh Ramalingam. Assembly and reliability challenges in 3d integration of 28nm fpga die on a large high density 65nm passive interposer. In *2012 IEEE 62nd Electronic Components and Technology Conference*, pages 279–283, 2012.
- [14] Jack Choquette and Wish Gandhi. Nvidia A100 GPU: Performance & innovation for GPU computing. In *2020 IEEE Hot Chips 32 Symposium (HCS)*, pages 1–43. IEEE Computer Society, 2020.
- [15] Chia Chen Chou, Aamer Jaleel, and Moinuddin K Qureshi. Cameo: A two-level memory organization with capacity of main memory and flexibility of hardware-managed cache. In *47th IEEE/ACM International Symposium on Microarchitecture*, pages 1–12. IEEE, 2014.
- [16] Emilio G Cota, Paolo Mantovani, and Luca P Carloni. Exploiting private local memories to reduce the opportunity cost of accelerator integration. In *Proceedings of the 2016 International Conference on Supercomputing*, pages 1–12, 2016.
- [17] Vidushi Dadu, Sihao Liu, and Tony Nowatzki. Polygraph: Exposing the value of flexibility for graph processing accelerators. In *2021 ACM/IEEE 48th Annual International Symposium on Computer Architecture (ISCA)*, pages 595–608. IEEE, 2021.
- [18] Jeffrey Dean and Sanjay Ghemawat. Mapreduce: simplified data processing on large clusters. *Communications of the ACM*, 51(11):107–113, 2008.
- [19] Yigit Demir, Yan Pan, Seukwoo Song, Nikos Hardavellas, John Kim, and Gokhan Memik. Galaxy: A high-performance energy-efficient multi-chip architecture using photonic interconnects. In *Proceedings of the 28th ACM international conference on Supercomputing*, pages 303–312, 2014.
- [20] Murali Emani, Venkatram Vishwanath, Corey Adams, Michael E Papka, Rick Stevens, Laura Florescu, Sumti Jairath, William Liu, Tejas Nama, and Arvind Sajeeth. Accelerating scientific applications with sambanova reconfigurable dataflow architecture. *Computing in Science & Engineering*, 23(2):114–119, 2021.
- [21] Esperanto Technologies. Esperanto's et-minion on-chip RISC-V cores. <https://www.esperanto.ai/technology/>.
- [22] Jessie Frazelle. Chip measuring contest: The benefits of purpose-built chips. *Queue*, 19(5):5–21, 2021.
- [23] Fei Gao, Ting-Jung Chang, Ang Li, Marcelo Orenes-Vera, Davide Giri, Paul J. Jackson, August Ning, Georgios Tziantzioulis, Joseph Zuckerman, Jinzheng Tu, Kaifeng Xu, Grigory Chirkov, Gabriele Tombesi, Jonathan Balkind, Margaret Martonosi, Luca Carloni, and David Wentzlaff. Decades: A 67mm², 1.46tops, 55 giga cache-coherent 64-bit RISC-V instructions per second, heterogeneous manycore soc with 109 tiles including accelerators, intelligent storage, and efgpa in 12nm finfet. In *Custom Integrated Circuits Conference (CICC)*, pages 1–2, 2023.
- [24] Saugata Ghose, Abdullah Giray Yaglikçi, Raghav Gupta, Donghyuk Lee, Kais Kudrolli, William X Liu, Hasan Hassan, Kevin K Chang, Niladrish Chatterjee, Aditya Agrawal, et al. What your dram power models are not telling you: Lessons from a detailed experimental study. *Proceedings of the ACM on Measurement and Analysis of Computing Systems*, 2(3):1–41, 2018.
- [25] Davide Giri, Kuan-Lin Chiu, Giuseppe Di Guglielmo, Paolo Mantovani, and Luca P. Carloni. ESP4ML: Platform-based design of systems-on-chip for embedded machine learning. In *DATE*. IEEE Press, 2020.
- [26] Wilfred Gomes, Altug Koker, Pat Stover, Doug Ingerly, Scott Siers, Srikrishnan Venkataraman, Chris Peltó, Tejas Shah, Amreesh Rao, Frank O'Mahony, et al. Ponte vecchio: A multi-tile 3d stacked processor for exascale computing. In *2022 IEEE International Solid-State Circuits Conference (ISSCC)*, volume 65, pages 42–44. IEEE, 2022.
- [27] Linley Gwennap. Groq rocks neural networks. *Microprocessor Report, Tech. Rep.*, jan, 2020.
- [28] Tae Jun Ham, Lisa Wu, Narayanan Sundaram, Nadathur Satish, and Margaret Martonosi. Graphiconado: A high-performance and energy-efficient accelerator for graph analytics. In *Proceedings of the 49th Annual International Symposium on Microarchitecture, MICRO*, 2016.
- [29] William Harrod. Agile: The future of data centric computing, 2022. https://www.youtube.com/watch?v=qIM_RBXX600.
- [30] High-Bandwidth Memory (HBM), 2015. <https://www.amd.com/Documents/High-Bandwidth-Memory-HBM.pdf>.
- [31] Intel. Intel Kaby Lake G, 2018. https://en.wikichip.org/wiki/intel/cores/kaby_lake_g.
- [32] JEDEC. Standard high bandwidth memory specification jesd235a, 2015.
- [33] Mark C. Jeffrey, Suvinay Subramanian, Cong Yan, Joel Emer, and Daniel Sanchez. A scalable architecture for ordered parallelism. In *Proceedings of the 48th International Symposium on Microarchitecture, MICRO-48*, page 228–241, New York, NY, USA, 2015. Association for Computing Machinery.
- [34] Scotten W. Jones. Lithovision: Economics in the 3d era. <https://semiwiki.com/wp-content/uploads/2020/03/Lithovision-2020.pdf>.
- [35] Norman P Jouppi, Cliff Young, Nishant Patil, David Patterson, Gaurav Agrawal, Raminder Bajwa, Sarah Bates, Suresh Bhatia, Nan Boden, Al Borchers, et al. In-datacenter performance analysis of a tensor processing unit. In *Proceedings of the 44th annual international symposium on computer architecture*, pages 1–12, 2017.
- [36] George Karypis and Vipin Kumar. Metis: A software package for partitioning unstructured graphs. *Partitioning Meshes, and Computing Fill-Reducing Orderings of Sparse Matrices, Version*, 4(0), 1998.
- [37] Dae-Hyun Kim, Byungkyu Song, Hyun-a Ahn, Woongjoon Ko, Sunggeun Do, Seokjin Cho, Kihan Kim, Seung-Hoon Oh, Hye-Yoon Joo, Geuntae Park, Jin-Hun Jang, Yong-Hun Kim, Donghun Lee, Jaehoon Jung, Yongmin Kwon, Youngjae Kim, Jaewoo Jung, Seongil O, Seoulmin Lee, Jaeseong Lim, Junho Son, Jisu Min, Haebin Do, Jaejun Yoon, Isak Hwang, Jinsol Park, Hong Shim, Seryeong Yoon, Dongyeong Choi, Jihoon Lee, Soohan Woo, Eunki Hong, Junha Choi, Jae-Sung Kim, Sangkeun Han, Jongmin Bang, Bokguk Park, Janghoo Kim, Seouk-Kyu Choi, Gong-Heum Han, Yoo-Chang Sung, Won-Il Bae, Jeong-Don Lim, Seungjae Lee, Changsik Yoo, Sang Joon Hwang, and Jooyoung Lee. A 16gb 9.5gb/s/pin lppdr5x sdram with low-power schemes exploiting dynamic voltage-frequency scaling and offset-calibrated readout sense amplifiers in a fourth generation 10nm dram process. In *2022 IEEE International Solid-State Circuits Conference (ISSCC)*, volume 65, pages 448–450, 2022.

- [38] Seongguk Kim, Subin Kim, Kyungjun Cho, Taein Shin, Hyunwook Park, Daehwan Lho, Shinyoung Park, Kyungjune Son, Gapyeol Park, and Joungho Kim. Processing-in-memory in high bandwidth memory (pim-hbm) architecture with energy-efficient and low latency channels for high bandwidth system. In *2019 IEEE 28th Conference on Electrical Performance of Electronic Packaging and Systems (EPEPS)*, pages 1–3, 2019.
- [39] Simon Knowles. Graphcore. In *2021 IEEE Hot Chips 33 Symposium (HCS)*, pages 1–25. IEEE, 2021.
- [40] Snehasish Kumar, Hongzhou Zhao, Arrvindh Shriraman, Eric Matthews, Sandhya Dwarkadas, and Lesley Shannon. Amoeba-cache: Adaptive blocks for eliminating waste in the memory hierarchy. In *45th Annual IEEE/ACM International Symposium on Microarchitecture*, pages 376–388. IEEE, 2012.
- [41] John H Lau. Status and outlooks of flip chip technology. *IPC EXPO Proceedings, February 2017*, pages 1–20, 2017.
- [42] Page Lawrence, Brin Sergey, Rajeev Motwani, and Terry Winograd. The PageRank citation ranking: Bringing order to the web. Technical report, Stanford University, 1998.
- [43] Chang-Chi Lee, Cp Hung, Calvin Cheung, Ping-Feng Yang, Chin-Li Kao, Dao-Long Chen, Meng-Kai Shih, Chien-Lin Chang Chien, Yu-Hsiang Hsiao, Li-Chieh Chen, Michael Su, Michael Alfano, Joe Siegel, Julius Din, and Bryan Black. An overview of the development of a gpu with integrated hbm on silicon interposer. In *2016 IEEE 66th Electronic Components and Technology Conference (ECTC)*, pages 1439–1444, 2016.
- [44] Dong Uk Lee, Ho Sung Cho, Jihwan Kim, Young Jun Ku, Sangmuk Oh, Chul Dae Kim, Hyun Woo Kim, Woo Young Lee, Tae Kyun Kim, Tae Sik Yun, et al. 22.3 a 128gb 8-high 512gb/s hbm2e dram with a pseudo quarter bank structure, power dispersion and an instruction-based at-speed pmibst. In *2020 IEEE International Solid-State Circuits Conference-(ISSCC)*, pages 334–336. IEEE, 2020.
- [45] Jure Leskovec, Deepayan Chakrabarti, Jon Kleinberg, Christos Faloutsos, and Zoubin Ghahramani. Kronecker graphs: An approach to modeling networks. *Journal of Machine Learning Research (JMLR)*, 11:985–1042, March 2010.
- [46] Cedric Lichtenau, Alper Buyuktosunoglu, Ramon Bertran, Peter Figuli, Christian Jacobi, Nikolaos Papandreou, Haris Pozidis, Anthony Saporito, Andrew Sica, and Elpidia Tzortzatos. AI accelerator on IBM telum processor: industrial product. In *Proceedings of the 49th Annual International Symposium on Computer Architecture*, pages 1012–1028, 2022.
- [47] Sean Lie. Multi-million core, multi-wafer AI cluster. In *2021 IEEE Hot Chips 33 Symposium*, pages 1–41. IEEE Computer Society, 2021.
- [48] Hang Liu and H Howie Huang. Enterprise: breadth-first graph traversal on gpus. In *International Conference for High Performance Computing, Networking, Storage and Analysis*, pages 1–12, 2015.
- [49] Ravi Mahajan, Robert Sankman, Neha Patel, Dae-Woo Kim, Kemal Aygun, Zhiguo Qian, Yidnekachew Mekonnen, Islam Salama, Sujit Sharan, Deepti Iyengar, et al. Embedded multi-die interconnect bridge (emib)—a high density, high bandwidth packaging interconnect. In *2016 IEEE 66th Electronic Components and Technology Conference (ECTC)*, pages 557–565. IEEE, 2016.
- [50] Aninda Manocha, Tyler Sorensen, Esin Tureci, Opeoluwa Matthews, Juan L Aragón, and Margaret Martonosi. Graphattack: Optimizing data supply for graph applications on in-order multicore architectures. *ACM Transactions on Architecture and Code Optimization (TACO)*, 18(4):1–26, 2021.
- [51] Roy Meade, Shahab Ardalan, Michael Davenport, John Fini, Chen Sun, Mark Wade, Alexandra Wright-Gladstein, and Chong Zhang. Teraphy: a high-density electronic-photonics chiplet for optical i/o from a multi-chip module. In *2019 Optical Fiber Communications Conference and Exhibition (OFC)*, pages 1–3. IEEE, 2019.
- [52] Micron. High Bandwidth Memory with ECC, 2018. https://media-www.micron.com/-/media/client/global/documents/products/data-sheet/dram/hbm2e/8gb_and_16gb_hbm2e_dram.pdf.
- [53] MooreElite. Die yield calculator. <http://cloud.mooreelite.com/tools/die-yield-calculator/index.html>.
- [54] Richard C. Murphy, Kyle B. Wheeler, Brian W. Barrett, and James A. Ang. Introducing the Graph 500. <http://www.graph500.org/specifications>, 2010.
- [55] Samuel Naffziger, Noah Beck, Thomas Burd, Kevin Lepak, Gabriel H. Loh, Mahesh Subramony, and Sean White. Pioneering chiplet technology and design for the amd epyc™ and ryzen™ processor families. In *Proceedings of the 48th Annual International Symposium on Computer Architecture*, ISCA '21, page 57–70. IEEE Press, 2021.
- [56] Nevine Nassif, Ashley O Munch, Carleton L Molnar, Gerald Pasdast, Sitaraman V Lyer, Zibing Yang, Oscar Mendoza, Mark Huddart, Srikrishnan Venkataraman, Sireesha Kandula, et al. Sapphire rapids: The next-generation intel xeon scalable processor. In *2022 IEEE International Solid-State Circuits Conference (ISSCC)*, volume 65, pages 44–46. IEEE, 2022.
- [57] Quan M Nguyen and Daniel Sanchez. Pipette: Improving core utilization on irregular applications through intra-core pipeline parallelism. In *2020 53rd Annual IEEE/ACM International Symposium on Microarchitecture (MICRO)*, pages 596–608. IEEE, 2020.
- [58] Quan M. Nguyen and Daniel Sanchez. Fifer: Practical acceleration of irregular applications on reconfigurable architectures. In *MICRO-54: 54th Annual IEEE/ACM International Symposium on Microarchitecture*, MICRO '21, page 1064–1077, New York, NY, USA, 2021. Association for Computing Machinery.
- [59] Chi-Sung Oh, Ki Chul Chun, Young-Yong Byun, Yong-Ki Kim, So-Young Kim, Yesin Ryu, Jaewon Park, Sinho Kim, Sanguhn Cha, Donghak Shin, et al. 22.1 a 1.1 v 16gb 640gb/s hbm2e dram with a data-bus window-extension technique and a synergetic on-die ecc scheme. In *2020 IEEE International Solid-State Circuits Conference-(ISSCC)*, pages 330–332. IEEE, 2020.
- [60] Open Compute Group. Bunch of wires phy specification. https://opencomputeproject.github.io/ODSA-BoW/bow_specification.html.
- [61] Marcelo Orenes-Vera, Aninda Manocha, Jonathan Balkind, Fei Gao, Juan L Aragón, David Wentzlaff, and Margaret Martonosi. Tiny but mighty: designing and realizing scalable latency tolerance for many-core socs. In *ISCA*, pages 817–830, 2022.
- [62] Marcelo Orenes-Vera, Ilya Sharapov, Robert Schreiber, Mathias Jacquelin, Philippe Vandermersch, and Sharan Chetlur. Wafer-scale fast fourier transforms. In *Proceedings of the 37th International Conference on Supercomputing*, ICS '23, page 180–191, New York, NY, USA, 2023. Association for Computing Machinery.
- [63] Marcelo Orenes-Vera, Esin Tureci, David Wentzlaff, and Margaret Martonosi. Dalorex: A data-local program execution and architecture for memory-bound applications. In *2023 IEEE International Symposium on High-Performance Computer Architecture (HPCA)*, pages 718–730. IEEE, 2023.
- [64] Marcelo Orenes-Vera, Esin Tureci, David Wentzlaff, and Margaret Martonosi. MuchiSim, 2023. <https://github.com/PrincetonUniversity/muchiSim.git>.
- [65] Muhammet Mustafa Ozdal, Serif Yesil, Taemin Kim, Andrey Ayupov, John Greth, Steven Burns, and Ozcan Ozturk. Energy efficient architecture for graph analytics accelerators. *ACM SIGARCH Computer Architecture News*, 44(3):166–177, 2016.
- [66] Mike O'Connor, Niladrish Chatterjee, Donghyuk Lee, John Wilson, Aditya Agrawal, Stephen W Keckler, and William J Dally. Fine-grained dram: Energy-efficient dram for extreme bandwidth systems. In *2017 50th Annual IEEE/ACM International Symposium on Microarchitecture (MICRO)*, pages 41–54. IEEE, 2017.
- [67] Saptadeep Pal, Daniel Petrisco, Matthew Tomei, Puneet Gupta, Subramanian S Iyer, and Rakesh Kumar. Architecting waferscale processors—a gpu case study. In *2019 IEEE International Symposium on High Performance Computer Architecture (HPCA)*, pages 250–263. IEEE, 2019.
- [68] Myeong-Jae Park, Ho Sung Cho, Tae-Sik Yun, Sangjin Byeon, Young Jun Koo, Sangsic Yoon, Dong Uk Lee, Seokwoo Choi, Jihwan Park, Jinhyung Lee, et al. A 192-gb 12-high 896-gb/s hbm3 dram with a tsv auto-calibration scheme and machine-learning-based layout optimization. In *2022 IEEE International Solid-State Circuits Conference (ISSCC)*, volume 65, pages 444–446. IEEE, 2022.
- [69] Andy Patrizio. High-bandwidth memory (hbm) delivers impressive performance gains. <https://semiengineering.com/whats-next-for-high-bandwidth-memory/>.
- [70] J Thomas Pawlowski. Hybrid memory cube (hmc). In *2011 IEEE Hot Chips 23 Symposium (HCS)*, pages 1–24. IEEE, 2011.
- [71] Gilead Posluns, Yan Zhu, Guowei Zhang, and Mark C. Jeffrey. A scalable architecture for reprioritizing ordered parallelism. In *Proceedings of the 49th Annual International Symposium on Computer Architecture*, ISCA '22, page 437–453, New York, NY, USA, 2022. Association for Computing Machinery.
- [72] CS Premachandran, Thuy Tran-Quinn, Lloyd Burrell, and Patrick Justison. A comprehensive wafer level reliability study on 65nm silicon interposer. In *2019 IEEE International Reliability Physics Symposium (IRPS)*, pages 1–8, 2019.
- [73] Valentin Puente, Ramón Beivide, José A Gregorio, JM Prellezo, Jose Duato, and Cruz Izu. Adaptive bubble router: a design to improve performance in torus networks. In *Proceedings of the 1999 International Conference on Parallel Processing*, pages 58–67. IEEE, 1999.

- [74] Shafiqur Rahman, Nael Abu-Ghazaleh, and Rajiv Gupta. Graphpulse: An event-driven hardware accelerator for asynchronous graph processing. In *2020 53rd Annual IEEE/ACM Symposium on Microarchitecture (MICRO)*, pages 908–921. IEEE, 2020.
- [75] Debendra Das Sharma. Pci express 6.0 specification: A low-latency, high-bandwidth, high-reliability, and cost-effective interconnect with 64.0 gt/s pam-4 signaling. *IEEE Micro*, 41(1), 2020.
- [76] Debendra Das Sharma, Gerald Pasdast, Zhiguo Qian, and Kemal Aygun. Universal chiplet interconnect express (ucie): An open industry standard for innovations with chiplets at package level. *IEEE Transactions on Components, Packaging and Manufacturing Technology*, 12(9):1423–1431, 2022.
- [77] Kota Shiba, Tatsuo Omori, Kodai Ueyoshi, Shinya Takamaeda-Yamazaki, Masato Motomura, Mototsugu Hamada, and Tadahiro Kuroda. A 96-mb 3d-stacked sram using inductive coupling with 0.4-v transmitter, termination scheme and 12: 1 serdes in 40-nm cmos. *IEEE Transactions on Circuits and Systems I*, 68(2):692–703, 2020.
- [78] George M. Slota, Sivasankaran Rajamanickam, and Kamesh Madduri. BFS and coloring-based parallel algorithms for strongly connected components and related problems. In *2014 IEEE 28th International Parallel and Distributed Processing Symposium, Phoenix, AZ, USA, May 19-23, 2014*, pages 550–559. IEEE Computer Society, 2014.
- [79] Kyomin Sohn, Won-Joo Yun, Reum Oh, Chi-Sung Oh, Seong-Young Seo, Min-Sang Park, Dong-Hak Shin, Won-Chang Jung, Sang-Hoon Shin, Je-Min Ryu, Hye-Seung Yu, Jae-Hun Jung, Hyunui Lee, Seok-Yong Kang, Young-Soo Sohn, Jung-Hwan Choi, Yong-Cheol Bae, Seong-Jin Jang, and Gyoyoung Jin. A 1.2 v 20 nm 307 gb/s hbm dram with at-speed wafer-level io test scheme and adaptive refresh considering temperature distribution. *IEEE Journal of Solid-State Circuits*, 52(1):250–260, 2017.
- [80] Dylan Stow, Yuan Xie, Taniya Siddiqua, and Gabriel H. Loh. Cost-effective design of scalable high-performance systems using active and passive interposers. In *2017 IEEE/ACM International Conference on Computer-Aided Design (ICCAD)*, pages 728–735, 2017.
- [81] John A Stratton, Christopher Rodrigues, I-Jui Sung, Nady Obeid, Li-Wen Chang, Nasser Anssari, Geng Daniel Liu, and W-m Hwu. Parboil: A revised benchmark suite for scientific and commercial throughput computing. Technical Report IMPACT-12-01, University of Illinois at Urbana-Champaign, 2012.
- [82] Raja Swaminathan and John Wuu. Chiplet’s march to amd 3d v-cache and beyond, 2022. <https://www.opencompute.org/events/past-events/hipchips-chiplet-workshop-isca-conference>.
- [83] Nishil Talati, Kyle May, Armand Behrooz, Yichen Yang, Kuba Kaszyk, Christos Vasiladiotis, Tarunesh Verma, Lu Li, Brandon Nguyen, Jiawen Sun, John Magnus Morton, Agreeen Ahmadi, Todd Austin, Michael O’Boyle, Scott Mahlke, Trevor Mudge, and Ronald Dreslinski. Prodigy: Improving the memory latency of data-indirect irregular workloads using hardware-software co-design. In *2021 IEEE International Symposium on High-Performance Computer Architecture (HPCA)*, pages 654–667. IEEE, 2021.
- [84] Emil Talpes, Douglas Williams, and Debjit Das Sarma. Dojo: The microarchitecture of tesla exa-scale computer. In *2022 IEEE Hot Chips 34 Symposium*, pages 1–28. IEEE Computer Society, 2022.
- [85] Tianqi Tang and Yuan Xie. Cost-aware exploration for chiplet-based architecture with advanced packaging technologies. *arXiv preprint arXiv:2206.07308*, 2022.
- [86] Yuanyuan Tian, Andrey Balmin, Severin Andreas Corsten, Shirish Tatikonda, and John McPherson. From "think like a vertex" to "think like a graph". *Proceedings of the VLDB Endowment*, 7(3):193–204, 2013.
- [87] Yangzihao Wang, Andrew Davidson, Yuechao Pan, Yuduo Wu, Andy Riffel, and John D Owens. Gunrock: A high-performance graph processing library on the gpu. In *Proceedings of the 21st ACM SIGPLAN symposium on principles and practice of parallel programming*, pages 1–12, 2016.
- [88] John Wilson. High-bandwidth density, energy-efficient, short-reach signaling that enables massively scalable parallelism, 2022. <https://www.opencompute.org/events/past-events/hipchips-chiplet-workshop-isca-conference>.
- [89] Yoshisato Yokoyama, Miki Tanaka, Koji Tanaka, Masao Morimoto, Makoto Yabuuchi, Yuichiro Ishii, and Shinji Tanaka. A 29.2 mb/mm² ultra high density sram macro using 7nm finfet technology with dual-edge driven wordline/bitline and write/read-assist circuit. In *2020 IEEE Symposium on VLSI Circuits*, pages 1–2, 2020.
- [90] F. Zaruba and L. Benini. The cost of application-class processing: Energy and performance analysis of a linux-ready 1.7-ghz 64-bit RISC-V core in 22-nm fdsoi technology. *IEEE Transactions on Very Large Scale Integration (VLSI) Systems*, 27(11):2629–2640, Nov 2019. <https://github.com/openhwgroup/cva6>.
- [91] Florian Zaruba, Fabian Schuiki, and Luca Benini. Mantcore: A 4096-core RISC-V chiplet architecture for ultraefficient floating-point computing. *IEEE Micro*, 41(2):36–42, 2020.
- [92] Mingxing Zhang, Youwei Zhuo, Chao Wang, Mingyu Gao, Yongwei Wu, Kang Chen, Christos Kozyrakis, and Xuehai Qian. Graphp: Reducing communication for pim-based graph processing with efficient data partition. In *2018 IEEE International Symposium on High Performance Computer Architecture (HPCA)*, pages 544–557. IEEE, 2018.
- [93] Youwei Zhuo, Chao Wang, Mingxing Zhang, Rui Wang, Dimin Niu, Yanzhi Wang, and Xuehai Qian. Graphq: Scalable pim-based graph processing. In *Proceedings of the 52nd Annual IEEE/ACM International Symposium on Microarchitecture*, pages 712–725, 2019.